Short Communication

Diketo acids inhibit the cap-snatching endonuclease of several *Bunyavirales*

Yaiza Fernández-García [a,*,1], Sebastiaan ter Horst [b,1], Marcella Bassetto [c], Andrea Brancale [d], Johan Neyts [b], Dominga Rogolino [e], Mario Sechi [f], Mauro Carcelli [e], Stephan Günther [a], Joana Rocha-Pereira [b,**]

[a] *Department of Virology, Bernhard-Nocht-Institute for Tropical Medicine, Hamburg, Germany*
[b] *KU Leuven, Rega Institute for Medical Research, Belgium*
[c] *Department of Chemistry, College of Science, Swansea University, United Kingdom*
[d] *Cardiff School of Pharmacy and Pharmaceutical Sciences, Cardiff University, United Kingdom*
[e] *Department of Chemistry, Life Sciences and Environmental Sustainability, University of Parma, Parco Area Delle Scienze, Parma, Italy*
[f] *Department of Chemistry and Pharmacy, Laboratory of Drug Design and Nanomedicine, University of Sassari, Italy*

ABSTRACT

Several fatal bunyavirus infections lack specific treatment. Here, we show that diketo acids engage a panel of bunyavirus cap-snatching endonucleases, inhibit their catalytic activity and reduce viral replication of a taxonomic representative *in vitro*. Specifically, the non-salt form of L-742,001 and its derivatives exhibited EC_{50} values between 5.6 and 6.9 μM against a recombinant BUNV-mCherry virus. Structural analysis and molecular docking simulations identified traits of both the class of chemical entities and the viral target that could help the design of novel, more potent molecules for the development of pan-bunyavirus antivirals.

The order *Bunyavirales* contains potentially fatal viruses that lack effective medical countermeasures. Many of them pose major public health threats and are pathogens prioritized in the World Health Organization (WHO) Blueprint for research and development (R&D) (Mehand et al., 2018). A hallmark is their segmented single-stranded RNA (ssRNA) genome with either negative or ambisense polarity. Thus, the synthesis of viral mRNA can be considered a limiting step in the early stages of the life cycle. The presence of 5′-capped extensions derived from the host mRNA in the viral transcripts suggests the use of a cap-snatching mechanism to initiate transcription. This mechanism was initially described for the *Influenza virus* (IFV) and although the specifics might vary between viruses, a constant feature is a metal dependent cap-snatching endonuclease (Cap-ENDO) responsible for the mRNA cleavage (Dias et al., 2009; Plotch et al., 1981; Reguera et al., 2016). Such viral enzymatic domain is essential for virus replication and presents a structurally conserved active site that can be exploited to generate broad-spectrum antivirals (Fernandez-Garcia et al., 2016; Reguera et al., 2010; Saez-Ayala et al., 2018; Song et al., 2016; Wang et al., 2020).

Very few data are available about the activity of bunyaviral Cap-ENDO inhibitors, but structural studies of the target support the idea that chelating agents as the class of diketo acids (DKAs) could be addressed as starting points for the creation of drug-like candidates (Jones et al., 2019; Reguera et al., 2010; Saez-Ayala et al., 2018). In this study, we assessed the inhibitory scope of a series of DKA compounds (Fig. 1) against Cap-ENDOs from several bunyaviruses. These small-molecules have proven to be effective inhibitors of metalloenzymes like the *Human Immunodeficiency virus 1* integrase (HIV-1 IN) and the IFV Cap-ENDO (Bacchi et al., 2011; Sechi et al., 2004; Stevaert et al., 2015), exerting their action through coordination to the bivalent metal ion(s) in the catalytic core of the enzymes. Particularly compound (8), also known as L-742,001, has demonstrated potent antiviral activity against IFV both *in vitro* and *in vivo* (Hastings et al., 1996; Nakazawa et al., 2008; Stevaert et al., 2015). It targets the two metal cofactors of the IFV Cap-ENDO via the DKA moiety while engaging crucial amino acids with its two aromatic "wings" (DuBois et al., 2012). Interestingly enough, although site-directed mutagenesis of residues associated to the active site of IFV Cap-ENDO leads to L-742,001 resistance, a single naturally emerging variant less susceptible to L-742,001 has been reported after serial passage of IFV in the presence of this molecule

---

* Corresponding author.
** Corresponding author.
E-mail addresses: fernandez-garcia@bnitm.de (Y. Fernández-García), joana.rochapereira@kuleuven.be (J. Rocha-Pereira).
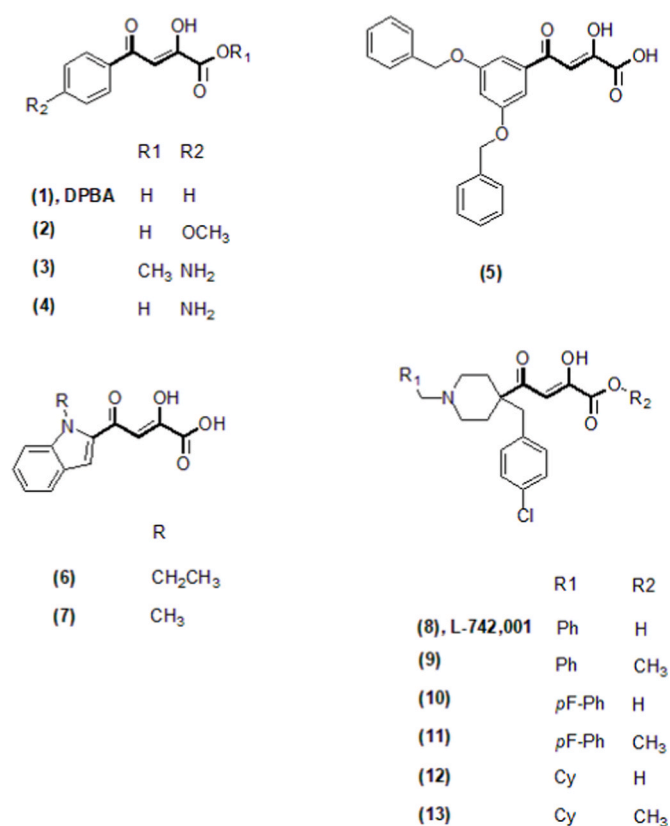[1] These authors contributed equally to this research.

Fig. 1. Schematic representation of compounds (1)–(13); in bold the chelating region.

(Nakazawa et al., 2008; Song et al., 2016; Stevaert et al., 2013). Compounds were obtained as previously reported (Bacchi et al., 2011; Maurin et al., 2004; Sanna et al., 2020; Sechi et al., 2004; Stevaert et al., 2015). The synthetic routes and the chemical characterization are described in the supplementary data.

A representative view of the compounds' effect over the taxonomic order was gathered using the biochemically active Cap-ENDOs of evolutionary divergent viruses. The wild-type (WT) domains of *La Crosse virus* (LACV; LACV_L$_{1-184}$_WT) and *Rift Valley Fever virus* (RVFV; RVFV_L$_{1-248}$_WT) were expressed and purified. Meanwhile, due to difficulties in the production of *Andes virus* (ANDV) soluble WT protein, we

chose mutant N167A (ANDV_L$_{1-200}$_N167A) as the best candidate to screen for small-molecule inhibitors. In contrast to the WT, ANDV_L$_{1-200}$_N167A can be expressed in bacteria, albeit retaining a considerable degree of nuclease activity. Residue 167 is located away from the catalytic pocket and the putative substrate-binding groove (Fernandez-Garcia et al., 2016). Proteins were produced as described in the supplementary data. To determine if the compounds were able to bind to the homologous enzymes, we measured the thermal stability of LACV_L$_{1-184}$_WT, RVFV_L$_{1-248}$_WT and ANDV_L$_{1-200}$_N167A in the presence of 25 μM of the corresponding DKA either with 10 mM EDTA or 10 mM MnCl$_2$. Only in the presence of the divalent cations, the compounds were able to contribute to the stability of the proteins, which is common for chelators that bind mainly through coordination to the metal cofactors. The highest increment to the melting temperature (Tm) in the presence of Mn^{2+} was observed with the addition of the prototype compound (8) and its salt L-742,001 hydrochloride (HCl), which raised the Tm (Δ Tm) by more than 5 °C in all Cap-ENDOs (Table 1; Fig. 2A). DKAs (8), (10), and (12) showed increments of the Tm bigger than the corresponding esters (9), (11), and (13), in accord with the higher complexing ability towards metal ions of the carboxyl group when compared to the ester group (Supplementary Fig. S1). Although the thermal shift assay (TSA) results might be in agreement with the ligands association constants, it can be misleading to rank compounds by their potency using the Δ Tm values (Lo et al., 2004; Pantoliano et al., 2001). Therefore, to evaluate the inhibitory capacity of DKAs, we further investigated the activity of all those that undoubtedly engaged the enzymes and exhibited a Δ Tm ≥ 3 °C.

A FRET-based nuclease-monitoring assay was employed to determine the half maximal inhibitory concentration (IC$_{50}$) of selected compounds. Serial dilutions of the respective compounds were preincubated for 15 min with 0.25 μM of the proteins in a mixture consisting of 50 mM Tris-HCl pH 7.5, 50 mM NaCl, 5% glycerol, 0.05 U/μl RNasin (Promega) and 10 mM MnCl$_2$ or EDTA. The reactions were initiated by the addition of 1 μM of a 12mer poly(A) ssRNA substrate labeled at the 5′ end with fluorophore 6-FAM and the 3′ end with quencher BHQ-1 purchased from Biomers. The fluorescence signal was measured every 10 s for 20 min in a 96-well plate format at wavelengths 490 nm and 515 nm for excitation and emission, respectively. The initial velocity of the reactions (V$_0$) was determined as the slope of the linear phase of the progress curves, and the percentages of the enzymatic activity were plotted against the concentrations of the compounds on a semilogarithmic graph. The IC$_{50}$ of the compounds was calculated by nonlinear regression analysis performed using GraphPad Prism version 7.00 (GraphPad Software, La Jolla California USA, www.graphpad.

Table 1
DKAs induced stability of *Bunyavirales* Cap-ENDO's and inhibitory potency.

Compound	Δ Tm (°C)			IC$_{50}$ (μM)		
	LACV L$_{1-184}$_WT	ANDV L$_{1-200}$_N167A	RVFV L$_{1-248}$_WT	LACV L$_{1-184}$_WT	ANDV L$_{1-200}$_N167A	RVFV L$_{1-248}$_WT
(1)	3.5 ± 0.5	4.9 ± 0.1	5.6 ± 0.2	24.9 ± 2.6	12.0 ± 1.7	2.8 ± 1.5
(2)	4.9 ± 0.3	3.5 ± 0.5	4.9 ± 0.03	29.8 ± 3.7	16.2 ± 2.8	5.7 ± 2.3
(3)	1.4 ± 0.01	1.4 ± 0.1	2.2 ± 0.1	NT	NT	NT
(4)	2.2 ± 0.8	2.9 ± 0.1	2.5 ± 1	NT	NT	NT
(5)	2.1 ± 0.2	1.9 ± 0.2	2.9 ± 0.1	NT	NT	NT
(6)	3 ± 0.3	2.1 ± 0.1	2.2 ± 0.2	NT	NT	NT
(7)	4.4 ± 0.1	3.2 ± 0.4	4.4 ± 0.3	31.0 ± 3.1	27.7 ± 4.1	11.1 ± 3.7
L-742,001 HCl	6.3 ± 0.3	6.4 ± 1	6.1 ± 0.2	4.0 ± 0.5	7.2 ± 0.5	10.2 ± 0.8
(8)	6.9 ± 0.9	6.1 ± 0.1	5.5 ± 0.3	7.3 ± 0.8	11.2 ± 1.7	13.9 ± 0.8
(9)	1.6 ± 0.4	0.4 ± 0.1	1.7 ± 0.3	NT	NT	NT
(10)	5 ± 0.8	4.1 ± 0.2	3.7 ± 0.6	13.7 ± 2.3	3.4 ± 0.5	11.9 ± 1.5
(11)	3.8 ± 0.5	2.6 ± 0.3	1.6 ± 0.3	NT	NT	NT
(12)	5.7 ± 0.1	4.3 ± 0.01	3.7 ± 0.1	11.4 ± 1.9	2.8 ± 0.5	11.4 ± 1.9
(13)	1.2 ± 0.8	2.8 ± 0.1	2.5 ± 0.3	NT	NT	NT

Δ Tm- The compound contribution to the enzyme thermal stability was determined by the difference in Tm between the samples containing MnCl$_2$ in the presence and absence of the respective compound; IC$_{50}$- The half-maximal inhibitory concentration was calculated by fitting the dose-response curves using a four parameter nonlinear regression; NT- Not tested. All data are mean ± standard deviation from 3 independent experiments.
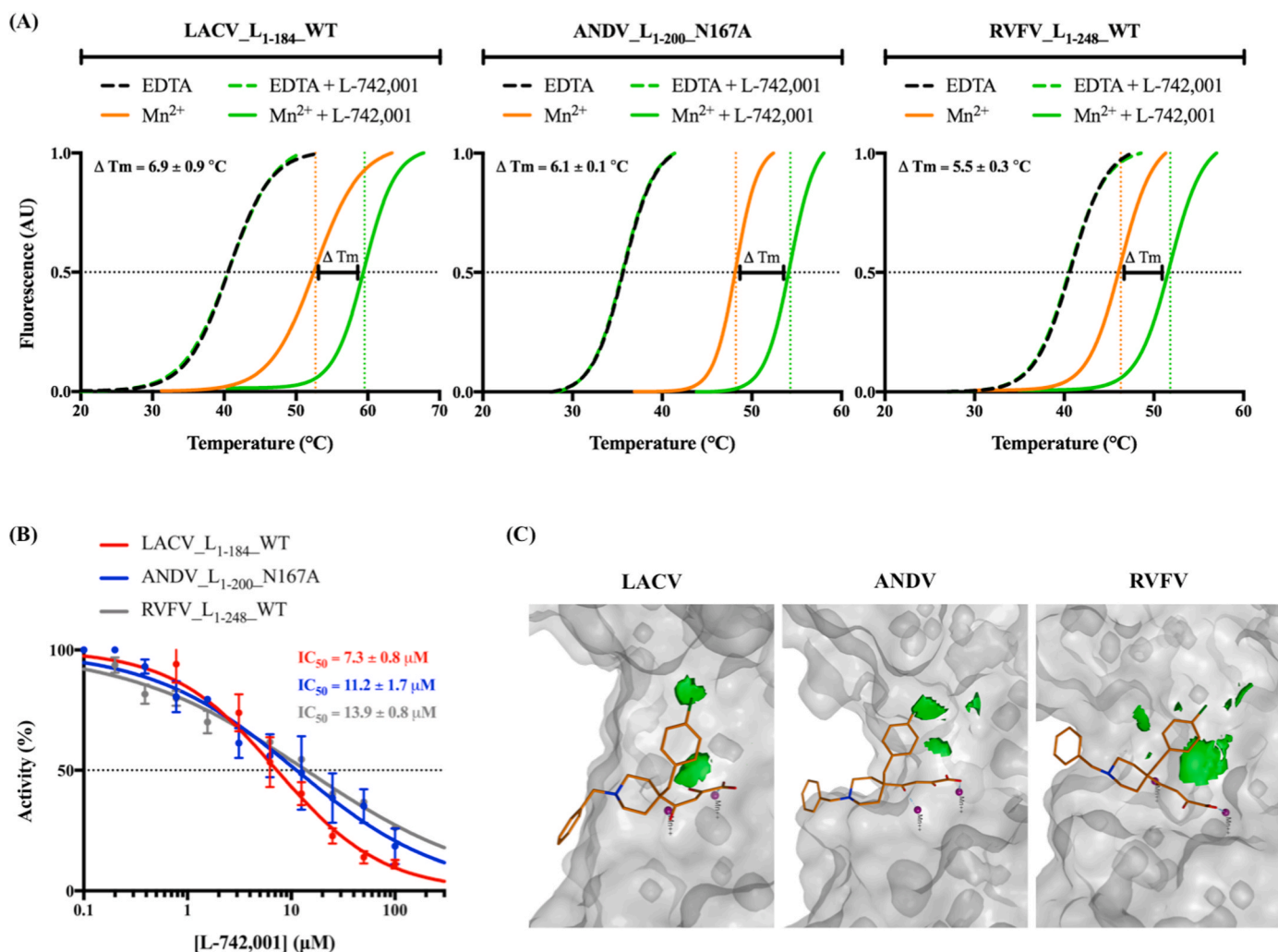
Fig. 2. L-742,001 inhibitory molecular interactions with *Bunyavirales* Cap-ENDO's. **(A)** Thermal stability of LACV_L$_{1-184}$_WT (left panel), ANDV_L$_{1-200}$_N167A (middle panel) and RVFV_L$_{1-248}$_WT (right panel) in the presence of 10 mM EDTA (black dashed line), 10 mM EDTA plus 25 μM L-742,001 (green dashed line), 10 mM MnCl$_2$ (orange solid line) and 10 mM MnCl$_2$ plus 25 μM L-742,001 (green solid line). The compound contribution to the stability of the proteins was determined by the difference in Tm between the samples containing MnCl$_2$ in the presence and absence of L-742,001 (Δ Tm). The lines depict the non-linear fits of the normalized fluorescence curves to the Boltzmann equation. **(B)** Dose-dependent inhibition of the nuclease activity of LACV_L$_{1-184}$_WT (red), ANDV_L$_{1-200}$_N167A (blue) and RVFV_L$_{1-248}$_WT (grey) by L-742,001. The reactions were initiated with the addition of 1 μM of FRET-labeled ssRNA substrate to the pre-incubated mixtures of 0.25 μM of the respective enzymes with two-fold serial dilutions of L-742,001. The fluorescent signal arising from the substrate cleavage was measured using a Roche LightCycler 480 II at λex/λem = 490 nm/515 nm. The V$_0$ of the reactions were used to calculate the percentage of activity at the different concentrations of the inhibitor. The dose-response curves were fit using a four parameter nonlinear regression. Δ Tm and half maximal inhibitory concentration (IC$_{50}$) values are the mean and standard deviation from 3 independent experiments. Final 5% DMSO concentration was maintained in all assays to favor compound solubility. **(C)** Molecular docking results for L-742,001 on the Cap-ENDOs of LACV (PDB: 2XI7), ANDV (PDB: 6Q99), and RVFV (homology model). All results are shown from the same orientation centered on the Mn^{2+} ions (purple), and display the similarities in the predicted binding between the different Cap-ENDOs. The hydrophobic contact area of a defined sub-pocket is represented in green.

com). (1) and its ester (2) as well as DKA (7) were able to suppress RVFV, ANDV and, to a lesser extent, also LACV Cap-ENDOs. Compounds (8) and its salt L-742,001 HCl, (10) and (12) were the most effective inhibitors of the RNA cleavage, displaying IC$_{50}$ values within the lower μM range towards all the Cap-ENDOs tested (Table 1). As shown for compound (8), all the DKAs tested had a similar dose-dependent effect over the catalytic activity of the different Cap-ENDOs (Fig. 2B).

In agreement with our results, L-742,001 has also been reported to inhibit the Cap-ENDO of the *Lymphocytic Choriomeningitis virus* (LCMV) (Saez-Ayala et al., 2018). The enzymatic domain of this other bunyavirus belongs to the subgroup of His - Cap-ENDOs, which characteristically possess a substantially reduced activity and are suggested to be regulated differently as the His + Cap-ENDOs used in this study (Holm et al., 2018). Thus, to investigate the binding of L-742,001 to the different Cap-ENDOs, we performed a series of molecular docking

experiments, using the available structures for LACV (PDB: 2XI7) and ANDV (PDB: 6Q99), and a homology model for RVFV (based on the TOSV Cap-ENDO structure; PDB: 6QVV). The results obtained indicate that, despite the overall structural similarity between the different Cap-ENDOs considered, the predicted L-742,001 binding region across the different proteins presents a degree of variability, both at a sequence and at a local structural level (Fig. 2C). Indeed, the main similarity is limited to the residues involved in the coordination of the Mn^{2+} ions. Overall, the binding site appears to be extensive and shallow. For this reason, there is a degree of variability in the binding of L-742,001 to the different enzymes. However, a common binding pattern, possibly indicating a common pharmacophore of three features, seems to emerge: the key interaction of the DKA with the Mn^{2+} ions through the ß-ketoacid group is maintained across the different structures, and it follows the same chelation geometry as observed in the crystallized LCMV/L-742,

001 complex; a common hydrophobic sub-pocket can be identified in the binding pocket, occupied by the chlorobenzyl ring of L-742,001 in all results obtained from the molecular docking as well as in the complex structure with LCMV domain (Supplementary Fig. S2); the tertiary amine of L-742,001 establishes a clear interaction respectively with Asp45 of the LACV Cap-ENDO and with Glu54 of the ANDV Cap-ENDO, while sits in the proximity of Asp62 in the RVFV Cap-ENDO model – all these three acidic residues are also involved in the coordination of an Mn^{2+} ion. These observations could potentially be exploited in the design of a novel series of more potent, broad-spectrum, Cap-ENDO inhibitors.

Having confirmed the inhibitory effect of L-742,001 and its salt L-742,001 HCl against a diverse set of bunyaviral Cap-ENDOs in enzymatic assays, we studied its ability to reduce viral replication in a cell-based assay. The antiviral activity against *Bunyamwera virus* (BUNV)-mCherry of L-742,001 HCl, L-742,001 and derivatives were evaluated in A549 cells (Shi et al., 2010). BUNV is considered a prototypic bunyavirus and is used as a model for research of pathogens within *Bunyavirales*. Serial dilutions of compounds were added followed by infection with 500 $CCID_{50}$ of virus. At 4 days post infection (dpi) cells were stained with a 2.5 µg/ml Hoechst solution and high content imaging analysis was performed on the Arrayscan XTI from Thermofisher® using a custom protocol based on the SpotDetector BioApplication (Cellomics® software). The cell nuclei were detected using a dynamic

threshold method based on differences in intensity peaks and the mCherry signal spots were detected by using a fixed intensity threshold based on the images acquired from the mCherry positive control (Fig. 3B). EC_{50} values are defined as the compound concentration that reduces the number of mCherry signal spots by 50% compared to the virus control (Fig. 3C). CC_{50} values are defined as the compound concentration that reduces the number of cells based on the nuclei by 50% compared to the virus control. In addition, we assessed the effect of the compounds on virus yield by RT-qPCR. Per reaction, a 20 µl RT-qPCR mix was prepared containing 4 µl of viral RNA with 600 nM and 900 nM of FW and REV primers, respectively (FW: 5′-ACACCACTGGGCTTAG-3′, REV: 5′-CAGCCCCCAAGGTTA-3′). For absolute quantification, standard curves were generated using 10-fold dilutions of template DNA of known concentration.

L-742,001 HCl inhibited BUNV-mCherry in a dose-dependent manner with EC_{50} values of 10.6 ± 1.6 µM and 18.5 ± 1.6 µM, as determined by high content imaging and RT-qPCR, respectively, with no cytotoxicity for the host cell ($CC_{50} > 100$ µM) (Fig. 3A). A similar profile was observed with the derivatives of L-742,001, both esters and carboxylic acids. Their EC_{50} is slightly lower than L-742,001 HCl, but although comparable to that of the parent non-salt form (Table 2). Unexpectedly, albeit presenting equivalent ^{1}H-NMR spectra (Supplementary Fig. S3), we observed higher cytotoxicity for the non-salt form of L-742,001 HCl.
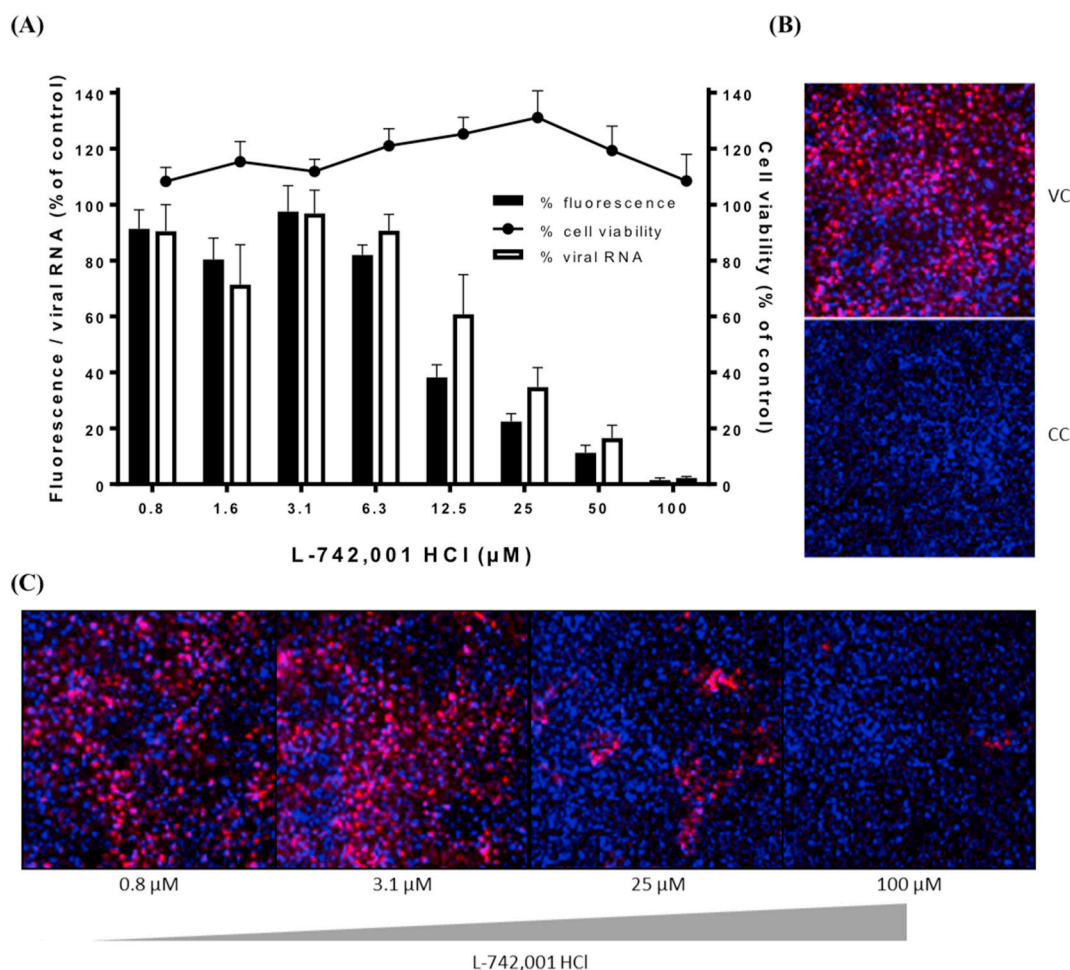

Fig. 3. L-742,001 *in vitro* antiviral activity against *Bunyaviruses*. **(A)** Effect of L-742,001 HCl on BUNV-mCherry replication in A549 cells. Viral mCherry signal spots (black bars) and cell viability (solid circles) were determined using high-content imaging analysis (n = 7). Viral RNA yield (white bars) were determined by RT-qPCR (n = 5). All data are mean ± standard deviation. **(B)** Representative images acquired through high content imaging of virus control (VC), cell control (CC). **(C)** Representative images acquired through high content imaging of BUNV-mCherry infected cells treated with a serial dilution of L-742,001 HCl. Images represent one out of nine fields acquired per well.

Table 2
Antiviral activity, viral yield, cytotoxicity and selectivity of L-742,001 HCl, L-742,001 and derivatives against BUNV-mCherry.

Compound	Antiviral activity EC_{50} (μM)	Viral RNA yield EC_{50} (μM)	Cytotoxicity CC_{50} (μM)	Selectivity index CC_{50}/EC_{50}
L-742,001 HCl	10.6 ± 1.6	18.5 ± 7.6	>100	>9.4
(8)	5.6 ± 1.8	6.6 ± 3.0	12.2 ± 2.9	2.2
(9)	6.9 ± 1.3	4.1 ± 0.4	11.2 ± 2.0	1.6
(10)	6.3 ± 1.1	12.3 ± 2.2	55.5 ± 13.1	8.8
(12)	6.3 ± 1.1	8.5 ± 0.5	42.7 ± 7.7	6.8
(13)	6.8 ± 2.0	9.7 ± 1.3	22.6 ± 3.4	3.3

EC_{50}- half-maximal effective concentration; CC_{50}- half-maximal cytotoxicity concentration. Antiviral activity and cytotoxicity were determined by high content imaging analysis (n = 6). Viral yield was determined by RT-qPCR (n = 3). All values, with exception of the selectivity index, are expressed as mean ± standard deviation.

In summary, our results demonstrate that the Cap-ENDO of bunyaviruses is a valid target for the development of broad-spectrum antivirals and that the DKAs class of compounds contains chemical features worth exploring in the design of novel inhibitors. We have documented the biochemical inhibition of several bunyaviral Cap-ENDOs by different DKAs and have confirmed that for a group of them, this translates to a modest antiviral activity as observed in the reduction of the number of mCherry spots and the viral RNA yield of the recombinant BUNV-mCherry virus. Moreover, our molecular docking simulations have provided us with some valuable information on the interaction of L-742,001 with this viral enzyme, defining a possible basic common pharmacophore for a broad-spectrum class of Cap-ENDO inhibitors. From these results, more potent and selective molecules with a wide range of action can now be designed. Hence, bringing us one step closer to a pan-bunyavirus antiviral.

Appendix A. Supplementary data

Supplementary data to this article can be found online at https://doi.org/10.1016/j.antiviral.2020.104947.

References

Bacchi, A., Carcelli, M., Compari, C., Fisicaro, E., Pala, N., Rispoli, G., Rogolino, D., Sanchez, T.W., Sechi, M., Neamati, N., 2011. HIV-1 in strand transfer chelating inhibitors: a focus on metal binding. Mol. Pharm. 8, 507–519. https://doi.org/10.1021/mp100343x.

Dias, A., Bouvier, D., Crépin, T., McCarthy, A., Hart, D.J., Baudin, F., Cusack, S., Ruigrok, R.W.H., 2009. The cap-snatching endonuclease of influenza virus polymerase resides in the PA subunit. Nature 458, 914–918. https://doi.org/10.1038/nature07745.

DuBois, R.M., Slavish, P.J., Baughman, B.M., Yun, M.K., Bao, J., Webby, R.J., Webb, T.R., White, S.W., 2012. Structural and biochemical basis for development of influenza virus inhibitors targeting the PA endonuclease. PLoS Pathog. 8 https://doi.org/10.1371/journal.ppat.1002830.

Fernandez-Garcia, Y., Reguera, J., Busch, C., Witte, G., Sanchez-Ramos, O., Betzel, C., Cusack, S., Günther, S., Reindl, S., 2016. Atomic structure and biochemical characterization of an RNA endonuclease in the N terminus of Andes virus L protein. PLoS Pathog. 12, 1–18. https://doi.org/10.1371/journal.ppat.1005635.

Hastings, J.C., Selnick, H., Wolanski, B., Tomassini, J.E., 1996. Anti-influenza virus activities of 4-substituted 2,4-dioxobutanoic acid inhibitors. Antimicrob. Agents Chemother. 40, 1304–1307. https://doi.org/10.1128/aac.40.5.1304.

Holm, T., Kopicki, J.D., Busch, C., Olschewski, S., Rosenthal, M., Uetrecht, C., Günther, S., Reindl, S., 2018. Biochemical and structural studies reveal differences and commonalities among cap-snatching endonucleases from segmented negative-strand RNA viruses. J. Biol. Chem. 293, 19686–19698. https://doi.org/10.1074/jbc.RA118.004373.

Jones, R., Lessoued, S., Meier, K., Devignot, S., Barata-García, S., Mate, M., Bragagnolo, G., Weber, F., Rosenthal, M., Reguera, J., 2019. Structure and function of the Toscana virus cap-snatching endonuclease. Nucleic Acids Res. 47, 10914–10930. https://doi.org/10.1093/nar/gkz838.

Lo, M.C., Aulabaugh, A., Jin, G., Cowling, R., Bard, J., Malamas, M., Ellestad, G., 2004. Evaluation of fluorescence-based thermal shift assays for hit identification in drug discovery. Anal. Biochem. 332, 153–159. https://doi.org/10.1016/j.ab.2004.04.031.

Maurin, C., Bailly, F., Cotelle, P., 2004. Improved preparation and structural investigation of 4-aryl-4-oxo-2- hydroxy-2-butenoic acids and methyl esters. Tetrahedron 60, 6479–6486. https://doi.org/10.1016/j.tet.2004.06.030.

Mehand, M.S., Al-Shorbaji, F., Millett, P., Murgue, B., 2018. The WHO R&D Blueprint: 2018 review of emerging infectious diseases requiring urgent research and development efforts. Antivir. Res. 159, 63–67. https://doi.org/10.1016/j.antiviral.2018.09.009.

Nakazawa, M., Kadowaki, S., Watanabe, I., Kadowaki, Y., Takei, M., Fukuda, H., 2008. PA subunit of RNA polymerase as a promising target for anti-influenza virus agents. Antivir. Res. 78, 194–201. https://doi.org/10.1016/j.antiviral.2007.12.010.

Pantoliano, M.W., Petrella, E.C., Kwasnoski, J.D., Lobanov, V.S., Myslik, J., Graf, E., Carver, T., Asel, E., Springer, B.A., Lane, P., Salemme, F.R., 2001. High-density miniaturized thermal shift assays as a general strategy for drug discovery. J. Biomol. Screen 6, 429–440. https://doi.org/10.1177/108705710100600609.

Plotch, S.J., Bouloy, M., Ulmanen, I., Krug, R.M., 1981. A unique cap(m7GpppXm)-dependent influenza virion endonuclease cleaves capped RNAs to generate the primers that initiate viral RNA transcription. Cell 23, 847–858. https://doi.org/10.1016/0092-8674(81)90449-9.

Reguera, J., Gerlach, P., Cusack, S., 2016. Towards a structural understanding of RNA synthesis by negative strand RNA viral polymerases. Curr. Opin. Struct. Biol. 36, 75–84. https://doi.org/10.1016/j.sbi.2016.01.002.

Reguera, J., Weber, F., Cusack, S., 2010. Bunyaviridae RNA polymerases (L-protein) have an N-terminal, influenza-like endonuclease domain, essential for viral cap-dependent transcription. PLoS Pathog. 6 https://doi.org/10.1371/journal.ppat.1001101.

Saez-Ayala, M., Yekwa, E.L., Carcelli, M., Canard, B., Alvareza, K., Ferron, F., 2018. Crystal structures of Lymphocytic choriomeningitis virus endonuclease domain complexed with diketo-acid ligands. IUCrJ 5, 223–235. https://doi.org/10.1107/S2052252518001021.

Sanna, V., Youssef, M.F., Pala, N., Rogolino, D., Carcelli, M., Singh, P.K., Sanchez, T., Neamati, N., Sechi, M., 2020. Inhibition of human immunodeficiency virus-1 integrase by β-diketo acid coated gold nanoparticles. ACS Med. Chem. Lett. https://doi.org/10.1021/acsmedchemlett.9b00648.

Sechi, M., Derudas, M., Dallocchio, R., Dessì, A., Bacchi, A., Sannia, L., Carta, F., Palomba, M., Ragab, O., Chan, C., Shoemaker, R., Sei, S., Dayam, R., Neamati, N., 2004. Design and synthesis of novel indole β-diketo acid derivatives as HIV-1 integrase inhibitors. J. Med. Chem. 47, 5298–5310. https://doi.org/10.1021/jm049944f.

Shi, X., van Mierlo, J.T., French, A., Elliott, R.M., 2010. Visualizing the replication cycle of Bunyamwera orthobunyavirus expressing fluorescent protein-tagged gc glycoprotein. J. Virol. 84, 8460–8469. https://doi.org/10.1128/jvi.00902-10.

Song, M.S., Kumar, G., Shadrick, W.R., Zhou, W., Jeevan, T., Li, Z., Slavish, P.J., Fabrizio, T.P., Yoon, S.W., Webb, T.R., Webby, R.J., White, S.W., 2016. Identification and characterization of influenza variants resistant to a viral endonuclease inhibitor. Proc. Natl. Acad. Sci. U. S. A 113, 3669–3674. https://doi.org/10.1073/pnas.1519772113.

Stevaert, A., Dallocchio, R., Dessi, A., Pala, N., Rogolino, D., Sechi, M., Naesens, L., 2013. Mutational analysis of the binding pockets of the diketo acid inhibitor L-742,001 in the influenza virus PA endonuclease. J. Virol. 87, 10524–10538. https://doi.org/10.1128/jvi.00832-13.

Stevaert, A., Nurra, S., Pala, N., Carcelli, M., Rogolino, D., Shepard, C., Domaoal, R.A., Kim, B., Alfonso-Prieto, M., Marras, S.A.E., Sechi, M., Naesens, L., 2015. An integrated biological approach to guide the development of metal-chelating inhibitors of influenza virus PA endonuclease. Mol. Pharmacol. 87, 323–337. https://doi.org/10.1124/mol.114.095588.

Wang, W., Shin, W.J., Zhang, B., Choi, Y., Yoo, J.S., Zimmerman, M.I., Frederick, T.E., Bowman, G.R., Gross, M.L., Leung, D.W., Jung, J.U., Amarasinghe, G.K., 2020. The cap-snatching SFTSV endonuclease domain is an antiviral target. Cell Rep. 30, 153–163. https://doi.org/10.1016/j.celrep.2019.12.020 e5.